

# Nanoscale

Accepted Manuscript



This is an *Accepted Manuscript*, which has been through the Royal Society of Chemistry peer review process and has been accepted for publication.

*Accepted Manuscripts* are published online shortly after acceptance, before technical editing, formatting and proof reading. Using this free service, authors can make their results available to the community, in citable form, before we publish the edited article. We will replace this *Accepted Manuscript* with the edited and formatted *Advance Article* as soon as it is available.

You can find more information about *Accepted Manuscripts* in the [Information for Authors](#).

Please note that technical editing may introduce minor changes to the text and/or graphics, which may alter content. The journal's standard [Terms & Conditions](#) and the [Ethical guidelines](#) still apply. In no event shall the Royal Society of Chemistry be held responsible for any errors or omissions in this *Accepted Manuscript* or any consequences arising from the use of any information it contains.



## Nanoscale

## COMMUNICATION

## White-Light-Emitting Magnetite Nanoparticle-Polymer Composites: Photonic Reactions of Magnetic Multi-Granule Nanoclusters as Photothermal Agents

Received 00th January 20xx,  
Accepted 00th January 20xx

DOI: 10.1039/x0xx00000x

www.rsc.org/

Yu Jin Kim,<sup>‡a</sup> Bum Chul Park,<sup>‡b</sup> June Park,<sup>c</sup> Hee-Dae Kim,<sup>d</sup> Nam Hoon Kim,<sup>e</sup> Yung Doug Suh<sup>\*e</sup> and Young Keun Kim<sup>\*b</sup>

1 Magnetite nanoparticles combined with polymers produce white  
2 light emission under multiphoton laser irradiation. Understanding  
3 the photonic reaction in magnetite-polymer composites is critical  
4 for application of the magnetite NPs as photothermal agents.  
5 Laser irradiated magnetite nanoparticles-poly(methyl  
6 methacrylate) (PMMA) composites exhibit fluorescence due to the  
7 carbon double-bond formation resulting from the oxidation of the  
8 PMMA.

9 Magnetic nanoparticles (NPs) are emerging as important  
10 multifunctional agents for various applications in  
11 nanobiotechnology, as well as memory devices due to their  
12 good superparamagnetism, favorable water dispersibility,  
13 properties, potentially good biocompatibility, and tailored  
14 surface chemistry.<sup>1-4</sup>  
15 Since most research efforts have been focused on the  
16 unique electromagnetic properties of magnetic NPs, their  
17 behavior under an electromagnetic field has been studied in  
18 detail.<sup>5,6</sup> However, the response of magnetic NPs to laser  
19 irradiation is not yet fully understood, since only a few studies  
20 on the phenomenological analysis of the photothermal and  
21 photodynamic therapies in the biomedical field have been  
22 reported to date.<sup>3,7-9</sup>

23 Recent research regarding the photothermal therapy has  
24 been focused on investigating reagents for the simultaneous  
25 therapy and *in vivo* imaging, most of which employ plasmonic

NPs.<sup>10-13</sup> The materials properties of efficient and stable photothermal agents must satisfy three conditions: large photon absorption cross-section, strong intraparticle interactions, and strong bonding to any surfactant.<sup>14</sup> Therefore, plasmonic gold (Au) NPs have been used in many systems as photothermal agents due to their adjustable optical characteristics, efficient heat generation, and potential biocompatibility.<sup>3,15-19</sup> However, Au NPs have a low luminous efficiency at a relatively strong absorption, and exhibit poor thermal stability due to the relatively weak metal-metal interactions at the high temperatures generated by the photothermal effect. These issues can cause variations in the NP distribution and morphology, as well as the destruction of the ligands attached to the Au NP surface, which will ultimately result in a loss of heat control at a molecular level from the photothermal Au NP-containing systems.<sup>14,20,21</sup> Moreover, nanosized Au can be a potential risk factor due to its accumulation inside the human body,<sup>22</sup> and thus, semiconductor NPs have been proposed as an alternative to Au NPs.<sup>23-25</sup> In particular, magnetite NPs exhibit better stability and *in vivo* compatibility than Au NPs at high temperature, and satisfy the required conditions for photothermal agents described earlier.<sup>14</sup> A recent study confirmed that magnetite NPs could be used as excellent photothermal agents due to their strong heat generation under NIR irradiation.<sup>8</sup> In a previous study, we reported the preparation of multifunctional magnetic NPs such as Fe<sub>3</sub>O<sub>4</sub>-ZnO core-shell NPs, self-assembly of Fe<sub>3</sub>O<sub>4</sub>-coordination polymer nanochains, and magnetic NPs conjugated with a photosensitizer.<sup>26-28</sup> Magnetic-PMMA composites are mainly used for the thermosensitive drug delivery and cell separation systems. They possess a high drug delivery efficiency due to their enhanced permeability, simple surface modification, surface stability, low toxicity, and *in vivo* biocompatibility.<sup>29,30</sup> In addition, PMMA-containing photodynamic systems produce photonic reactions due to a thermal effect. Therefore, understanding the characteristic variations of the magnetite NP-PMMA composites produced by the photothermal effect is essential.

<sup>a</sup> Center for Creative Materials and Components, Korea University, 145 Anam-ro, Seongbuk-gu, Seoul 02841, Korea.

<sup>b</sup> Department of Materials Science and Engineering, Korea University, 145 Anam-ro, Seongbuk-gu, Seoul 02841, Korea. E-mail: ykim97@korea.ac.kr; Fax: +82-2-928-3584; Tel: +82-2-3290-3281

<sup>c</sup> Ultra-Precision Optics Research Sector, Korea Photonics Technology Institute, Gwangju, 61007, Korea.

<sup>d</sup> Department of Biological Sciences, Seoul National University, Seoul 08826, Korea

<sup>e</sup> Research Center for Convergence NanoRaman Technology, Korea Research Institute of Chemical Technology, Yuseong, P.O. Box 107, Daejeon 34114, Korea. E-mail: ydsuh@kriict.re.kr; Fax: +82-42-860-7625; Tel: +82-42-860-7597

\* Y.K.K and Y.D.S developed and supervised the project.

Electronic Supplementary Information (ESI) available: Detail experimental procedures and additional results of photonic reactions are presented. See DOI: 10.1039/x0xx00000x

‡These authors made equal contributions to this study.

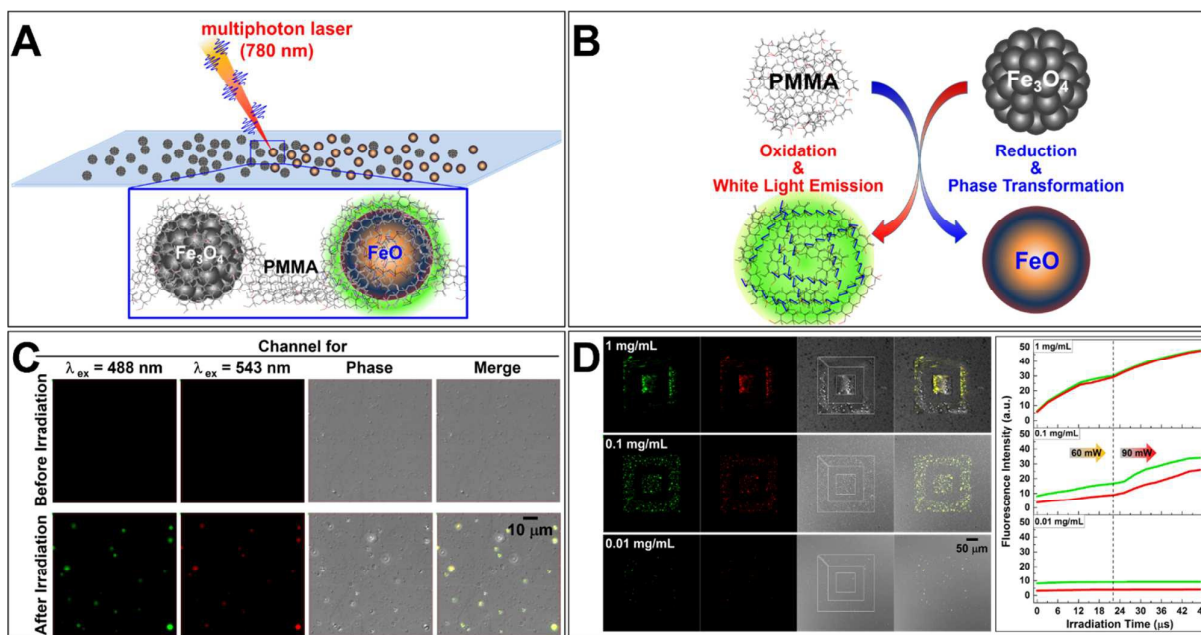


**Fig. 1** White light emission by the MGNC-PMMA composites under 780 nm multiphoton laser irradiation photonic stimulus. (A) A schematic representation of the photonic reaction of the MGNC-PMMA composites. (B) A diagram illustrating the photonic reaction in magnetite and PMMA polymers induced by the photothermal effect. (C) Fluorescent images of the MGNC-PMMA composites (concentration: 0.1 mg/mL) before and after the 780 nm multiphoton laser irradiation. (D) Emission intensity depends on the MGNC concentration. The fluorescent images depicted in panels C and D are measured at the magnifications of 100X and 20X, respectively; the areas inside the white boxes in panel D were partially subjected to irradiation by a 780 nm multiphoton laser.

1 PMMA is a well-known polymer that can undergo structural  
 2 modifications due to thermal stimulus and electron irradiation.  
 3 However, there are only a few studies on the stability and  
 4 properties of the magnetite-PMMA composites subjected to  
 5 photonic irradiation, while the investigation of the photonic  
 6 reactions of the magnetite-PMMA composites could be  
 7 beneficial for theranostic applications.<sup>7</sup>  
 8 In this study, we report the photothermal effects produced  
 9 by NIR-sensitive magnetic MGNC NP-polymer nanocomposites,  
 10 which result from the interaction between the magnetic multi-  
 11 granule nanoclusters (MGNCs; 100 nm in diameter) and the  
 12 780 nm multiphoton laser irradiation. We demonstrate for the  
 13 first time the generation of a strong luminescence under  
 14 photothermal effect-induced thermal degradation and  
 15 oxidation of the PMMA chains.  
 16 Multiphoton confocal microscopy (LSM 710 NLO confocal  
 17 microscope, Carl Zeiss) was used to investigate the MGNC-  
 18 polymer complexes. UV-visible spectroscopy (UV-Vis: UV-48  
 19 NIR spectrophotometer, Cary 5000, Agilent Technologies),  
 20 Raman spectroscopy (LabRam ARAMIS IR2, Horiba Jobin Yvon),  
 21 X-ray photoelectron spectroscopy (XPS: X-Tool, ULVAC-PHOTO  
 22 transmission electron microscopy (TEM: JEM-2100F, JEOL), a  
 23 X-ray diffraction (XRD: D/Max-2500, Rigaku) were used to  
 24 study the structural modifications of the nanocluster-polymer  
 25 complexes.  
 26 Figures 1A and B schematically describe the experimental  
 27 setup used for the white-light-emitting systems and the  
 28 photonic reactions (including oxidation of the PMMA polymer  
 29 and reduction of the MGNC) of the nanocomposites through  
 30 magnetite-based photothermal effect. The photothermal

effect of magnetite induced by the 780 nm multiphoton laser  
 irradiation results in a continuous heat generation; and the  
 oxidation, resulting in thermal degradation of the PMMA  
 polymer around the particles, leads to the emission of green  
 and red luminescence (Figure 1C). Figure 1D displays the  
 differences in luminescence intensity using different particle  
 concentrations indicating that the latter is an important factor  
 in determining the light emission intensity under multiphoton  
 laser irradiation with a constant power intensity. After  
 different compounds were tested under these conditions, the  
 obtained fluorescence intensity in the visible range increased  
 with the PMMA degradation, which indicates that the white-  
 light emitted by the PMMA is due to the creation of new  
 luminescence centers formed by the photothermal and  
 photochemical reactions. In order to investigate this previously  
 unknown phenomenon, various conditions were studied.  
 However, no significant emission was observed for both the  
 PMMA and Au NP-PMMA composites using low-power  
 multiphoton laser irradiation (Figure 2A and B). In particular,  
 the MGNC-PMMA composites present a green and red  
 fluorescence intensity 10 times stronger than that of the Au  
 NPs-PMMA composites and PMMA after 60 mW irradiation  
 using a 780 nm multiphoton laser.

The Au NPs also emit luminescence due to the  
 photothermal effect, but they require significantly higher  
 levels of multiphoton laser irradiation (10 times stronger or  
 more). These results indicate that the white-light emission  
 originates from the thermal degradation and oxidation of the  
 PMMA depending on the heat generation of the laser-  
 irradiated sample. In addition, the light emission shown by the

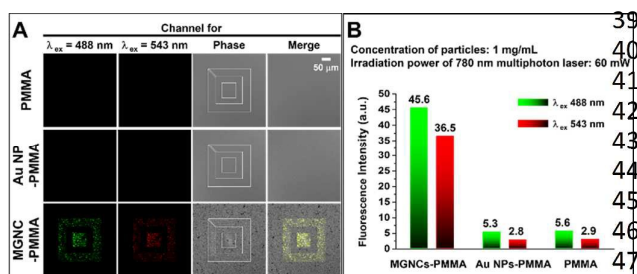


**Fig. 2** Comparison of the fluorescence emission properties for various composite materials. (A) In contrast to the PMMA and Au-PMMA composites, the MGNC-PMMA composites were luminous in the entire visible range under identical irradiation conditions (780 nm multiphoton laser power: 60 mW) (top row: PMMA, mid row: 1 mg/mL of the Au-PMMA composites, bottom row: 1 mg/mL of the MGNC-PMMA composites). (B) Fluorescence intensities of the MGNC-PMMA composites, Au NP-PMMA composites, and PMMA polymer, respectively, under identical conditions.

1 PMMA and Au NP-PMMA composites is produced by the  
 2 multiphoton laser irradiation, which requires higher energy  
 3 than those for the MGNC-PMMA composites (see Electronic  
 4 Supporting Information, Figure S1). Thus, magnetite NPs can  
 5 be used as efficient heat-generating agents due to their ability  
 6 to accumulate energy under low-power 780 nm multiphoton  
 7 laser irradiation.

8 The heat generation due to the photothermal effect of the  
 9 magnetite NPs and the reduction of Fe ions in magnetite NPs  
 10 together with the oxidation of PMMA polymer imparted  
 11 morphological and crystal structure modifications to the  
 12 granule cluster particles from magnetite ( $\text{Fe}_3\text{O}_4$ ) to wüstite  
 13 ( $\text{FeO}$ ). The transformation of the metastable wüstite phase  
 14 after the 780 nm multiphoton laser irradiation was confirmed  
 15 using XRD analysis (Figures 3A and B). The TEM measurements  
 16 reveal a morphological and crystallographic structural  
 17 modification in the MGNCs (Figure 3A), showing that the  
 18 MGNC characteristics corresponding to the multi-granule  
 19 geometric and polycrystalline structures disappear after the  
 20 780 nm multiphoton laser irradiation, which is possibly due to  
 21 a modification of the MGNCs phase or composition. The  
 22 observed crystallization results from the conformational  
 23 changes due to sintering at high-temperature. The XRD  
 24 analysis (Figure 3B) shows a noticeable increase in the (200)  
 25 peak intensity and decrease in the (311) peak intensity after  
 26 irradiation, which correspond to the wüstite and magnetite  
 27 phases, respectively.<sup>31</sup> This is consistent with the heat  
 28 generation by the MGNCs due to the low-power 780 nm  
 29 multiphoton laser irradiation (the overall relative intensities of  
 30 the other XRD peaks remained mostly unchanged). The  
 31 temperature near the focusing area was elevated high enough  
 32 to cause sintering and phase transformation when the  
 33 magnetite MGNCs absorbed laser energy. As previously  
 34 known, the phase transformation from magnetite to wüstite  
 35 requires high temperature, and sintering process of magnetite  
 36 granules can occur below the phase transformation  
 37 temperature.<sup>32</sup> In case of our experiments, PMMA polymer  
 38 which covers the surface of magnetite nanoparticles can

induce reduction of magnetite nanoparticles to wüstite  
 nanoparticle with phase transformation.

Furthermore, the observed luminescence can be explained  
 by the fact that the excitation wavelength-dependent  
 luminescence spectra reflects the distribution of the emission  
 sites interacting with the carbon chains of the thermally  
 deformed PMMA polymers. It has been recently reported that  
 the white-light emission originates from the band gap created  
 by possible modifications or recombination of the carbon  
 chains.<sup>33-35</sup>

It has been reported that carbon nanostructures are  
 characterized by high fluorescence quantum yields produced  
 by irradiation in the ultraviolet region, and thus exhibit an  
 excitation wavelength-dependency with the fluorescence  
 emission intensity.<sup>36,37</sup>

Therefore, the thermal degradation and oxidation of the  
 carbon bonds in the PMMA species attached to the MGNC  
 surface are strongly correlated with the luminescence emitted  
 over the entire visible range. To investigate this luminescence  
 in more detail, the UV-Vis absorption and photoluminescence  
 (PL) emission spectra of the MGNC-PMMA composites were  
 measured using a UV laser as the excitation source. As shown  
 in Figure 3C, the PMMA and MGNC-PMMA films before  
 irradiation are characterized by lower absorbance values than  
 those obtained with the multiphoton laser irradiated MGNC-  
 PMMA composite films. However, the latter exhibit a  
 significant increase in the absorption intensity in the region  
 between 380 and 600 nm, which indicates the creation of a

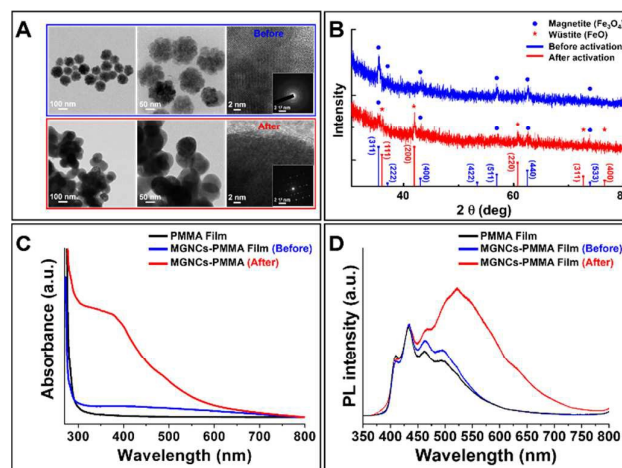


**Fig. 3** Structural and optical analysis of the MGNC-PMMA composites before (blue lines) and after (red lines) the laser irradiation. (A) TEM images of the MGNCs. (inset is a selected area electron diffraction pattern from both of MGNCs before and after irradiation) (B) XRD patterns of the MGNC-PMMA composites. The magnetite (JCPDS No. 19-0629) and wüstite (JCPDS No. 46-1312) peak positions are denoted in the bottom part of the figure by the blue and red vertical lines, respectively. (C) UV-Visible absorption spectra of the MGNC-PMMA composites and PMMA film. (D) PL spectra of the MGNC-PMMA composites and PMMA film at the excitation wavelength of 325 nm.

new electronic band structure with distinctive luminous  
 characteristics for the multiphoton laser irradiated MGNC-  
 PMMA composite films.<sup>34</sup>

To study the optical properties of the MGNC-PMMA composites, PL experiments were performed in the range between 400 and 800 nm using a 325-nm He-Cd laser. Figure 3D shows the PL spectra for the PMMA and MGNC-PMMA composite films before and after the multiphoton laser irradiation. The MGNC-PMMA composite after irradiation uniquely characterized by a broad PL peak spreading across the entire visible light region and centered at 520 nm, which is very similar to the one previously reported for carbon-based nanostructures.<sup>33,36</sup> The emission across the entire visible range spectrum can be explained by the formation of conjugated chemical bonds in the polymers under irradiation.<sup>38</sup> Thus, this drastic absorption increase in the UV-Vis range (Figure 3C) can result from the formation of structures associated with a new carbon bond state corresponding to the broad PL spectrum. In order to determine whether the luminescence was produced by the modifications in the carbon chains, the conformational changes in the PMMA polymer have to be analyzed.

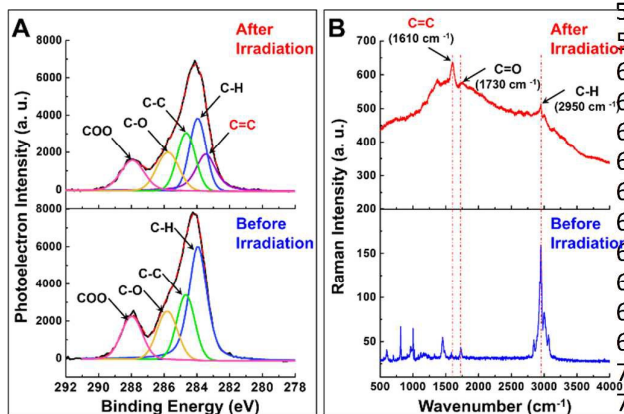


**Fig. 4** (A) XPS C 1s spectra of the MGNC-PMMA composites before and after the laser irradiation. (B) Raman spectra of the MGNC-PMMA composites before (blue lines) and after (red lines) the laser irradiation.

To confirm the formation of  $\pi$ - $\pi$  bonding, XPS spectra of the nanocomposites were obtained before and after the 780 nm multiphoton laser irradiation (Figure 4A). The observed variations in the main C 1s peak centered at a binding energy of 283.46 eV indicate that the intensity of the C=C bond increased after the 780 nm multiphoton laser irradiation, while the intensities of the other carbon components decreased. The obtained XPS results suggest that the photonic reaction of the polymer under the 780 nm multiphoton laser irradiation leads to cleavages of both C-C and C-H bonds with the subsequent formation of C=C bonds from thermal degradation, which in turn result in  $\pi$ -conjugation. Thus, the white-light emission (with a maximum centered at 520 nm) can be attributed to the formation of C=C bonds resulting from the polymer degradation on the surface of the magnetic NPs.

To demonstrate further the carbon bonds of the sample, Raman spectra of the MGNC-PMMA composite were obtained before and after the 780 nm multiphoton laser irradiation (Figure 4B). Supporting the XPS analysis, Raman measurement

allows to determine the variation of C=C bonding between both of the MGNC-PMMA composites. Raman signatures exhibit a powerful ability to verify the vibrational symmetric stretch of functional group such as the C=C bond. Moreover, the Raman signatures of PMMA polymer are established well. In figure 4B (lower graph), there are several Raman signatures for the PMMA polymer at 601  $\text{cm}^{-1}$  ( $\nu(\text{C-COO})$ ), 809  $\text{cm}^{-1}$  ( $\nu(\text{C-COO})$ ), 967  $\text{cm}^{-1}$  ( $\nu(\text{C-COO})$ ), 995  $\text{cm}^{-1}$  ( $\nu(\text{O-CH}_3)$ ), 1452  $\text{cm}^{-1}$  ( $\delta_a(\text{C-H})$  of  $\alpha\text{-CH}_3$ ,  $\delta_a(\text{C-H})$  of  $\text{O-CH}_3$ ), and 2950  $\text{cm}^{-1}$  ( $\nu_s(\text{C-H})$  of  $\text{O-CH}_3$ ,  $\nu_s(\text{C-H})$  of  $\alpha\text{-CH}_3$ , and  $\nu_a(\text{CH}_2)$ ).<sup>39</sup> Specifically, Raman signatures assigned to C=C bonds and carbonyl functional groups exhibited a substantial variation at 1610 and 1730  $\text{cm}^{-1}$ , respectively. A Raman spectrum of irradiated MGNC-PMMA composites shows broad baseline in Figure 4B (upper graph). Because the Raman spectrum was obtained using 532 nm laser as an excitation source, the broad baseline is photoluminescence background from the irradiated sample. Nevertheless, Figure 4B (upper graph) shows the Raman signature at around 1610  $\text{cm}^{-1}$ , assigned to the carbon  $sp^2$  bonding, which increases remarkably after the 780 nm multiphoton laser irradiation<sup>40</sup> indicating that the rearrangement of the polyacetylene-like backbone chains (C=C bonding) in  $\pi$ -conjugated polymers promotes the formation of  $\pi$ - $\pi$  bonding structures, while the conjugated chemical bonding in polymers might produce a white-light emission under UV irradiation.<sup>38</sup> Thus, the formation and rearrangement of the  $\pi$ -conjugated polymer chains are caused by the interaction between the MGNCs and PMMA polymer in the MGNC-PMMA composite irradiated by the 780 nm multiphoton laser (see Electronic Supporting Information, Figure S2).

In this study, we demonstrated that the white-light emission of a MGNC-PMMA composite could be enhanced by multiphoton laser-related interactions. The 780 nm multiphoton laser-irradiated MGNC-PMMA composites emit a bright full-spectrum visible light with a dominant peak at 525 nm, which is associated to the formation of C=C bonds due to the photothermal and photochemical transformations of the polymer. The mechanism of this white-light emission is not yet fully understood; however, the  $\pi$ -conjugation induced by the polymer degradation, as well as the PMMA chain oxidation under the influence of the heat generated due to the photothermal effect of the MGNCs can be suggested.

The MGNCs can widen the scope of applications using the photothermal therapy because they possess excellent heat-generation properties with non-invasive and good penetration characteristics under low-power 780 nm multiphoton laser irradiation. The findings reported in this study suggest that the MGNCs can be potentially used as efficient photothermal agents in the field of cancer therapy. In addition, the generation of white-light by the MGNC-polymer composites can offer new strategies for the preparation of flexible displays and photovoltaic devices.

## Acknowledgments

- 1 Y.K.K. was supported by the Nano-Material Technology  
 2 Development Program through the National Research  
 3 Foundation of Korea funded by the Ministry of Science,  
 4 and Future Planning (Grant No. 2014M3A7B4052193). Y.D.  
 5 was supported by KRICT (SI-1509, KK-1603-A0) and the Degr  
 6 and Research Center (DRC) Program (2015) through  
 7 National Research Council of Science & Technology (NST) fro  
 8 the Ministry of Science, ICT and Future Planning. Y.J.K. wa  
 9 supported by the Basic Science Research Program through the  
 10 National Research Foundation of Korea funded by the Ministr  
 11 of Education (Grant No. NRF-2013R1A1A2063087). Y.J.K.  
 12 acknowledges the financial support from Korea University.
- 13 Notes and references**
- 14 1 U. Jeong, X. W. Teng, Y. Wang, H. Yang and Y. N. Xia, *Adv.*  
 15 *Mater.*, 2007, **19**, 33.  
 16 2 M. Liong, J. Lu, M. Kovochich, T. Xia, S. G. Ruehm, A. E. Nel,  
 17 Tamanoi and J. I. Zink, *ACS Nano*, 2008, **2**, 889.  
 18 3 W. Dong, Y. Li, D. Niu, Z. Ma, J. Gu, Y. Chen, W. Zhao, X. Liu,  
 19 C. Liu and J. Shi, *Adv. Mater.*, 2011, **23**, 5392.  
 20 4 J. Zhou, L. Meng, Q. Lu, J. Fu and X. Huang, *Chem. Commun.*  
 21 2009, **42**, 6370.  
 22 5 J. S. Lee, J. M. Cha, H. Y. Yoon, J. Lee and Y. K. Kim, *Sci. Rep.*  
 23 *UK*, 2015, **5**, 12135.  
 24 6 H. Zeng, C. T. Black, R. L. Sandstrom, P. M. Rice, C. B. Murray  
 25 and S. Sun, *Phys. Rev. B*, 2006, **73**, 020402.  
 26 7 R. A. Revia and M. Zhang, *Materials Today* 2015 (Online)  
 27 <http://dx.doi.org/10.1016/j.mattod.2015.08.022>.  
 28 8 M. Chu, Y. Shao, J. Peng, X. Dai, H. Li, Q. Wu and D. Shi,  
 29 *Biomaterials*, 2013, **34**, 4078.  
 30 9 S. Laurent, S. Dutz, U. O. Häfeli and M. Mahmoudi, *M. Adv.*  
 31 *Colloid. Interfac.*, 2011, **166**, 8.  
 32 10 X. D. Zhang, D. Wu, X. Shen, P. X. Liu, F. Y. Fan and S. J. Fan,  
 33 *Biomaterials*, 2012, **33**, 4628.  
 34 11 M. Longmire, P. L. Choyke and H. Kobayashi, *Nanomedicine*  
 35 2008, **3**, 703.  
 36 12 W. S. Cho, M. Cho, J. Jeong, M. Choi, B. S. Han, H. Shin, J.  
 37 Hong, B. H. Chung, J. Jeong and M. Cho, *Toxicol. Appl.*  
 38 *Pharmacol.*, 2010, **245**, 116.  
 39 13 Y. Pan, S. Neuss, A. Leifert, M. Fischler, F. Wen, U. Simon,  
 40 Schmid, W. Brandau and W. Jahnhen-Dechent, *Small*, 2007,  
 41 1941.  
 42 14 R. J. G. Johnson, K. M. Haas and B. J. Lear, *Chem. Commun.*  
 43 2015, **51**, 417.  
 44 15 E. C. Dreaden, M. A. Mackey, X. Huang, B. Kang and M. A.  
 45 Sayed, *Chem. Soc. Rev.*, 2011, **40**, 3391.  
 46 16 B. Kang, M. A. Mackey, and M. A. El-Sayed, *J. Am. Chem. Soc.*  
 47 2010, **132**, 1517.  
 48 17 A. Espinosa, A. K. A. Silva, A. Sanchez-Iglesias, M. Grzelczak,  
 49 C. Pechoux, K. Desboeufs, L. M. Liz-Marzan and C. Wilhelm,  
 50 *Adv. Healthcare Mater.*, 2016, **5**, 1040.  
 51 18 K. M. Haas and B. J. Lear, *Chem. Sci.*, 2015, **6**, 6462.  
 52 19 D. K. Lim, A. Barhoumi, R. G. Wylie, G. Reznor, R. S. Langer  
 53 and D. S. Kohane, *Nano Lett.*, 2013, **13**, 4075.  
 54 20 L. Poon, W. Zandberg, D. Hslao, Z. Erno, D. Sen, B. D. Gates  
 55 and N. R. Branda, *ACS Nano*, 2010, **4**, 6395.  
 56 21 E. Y. Hleb and D. O. Lapotko, *Nanotechnology*, 2008, **19**,  
 57 355702.  
 58 22 N. Khlebtsov and L. Dykman, *Chem. Soc. Rev.*, 2011, **40**,  
 59 1647.  
 60 23 W. Li, P. Rong, K. Yang, P. Huang, K. Sun and X. Chen,  
 61 *Biomaterials*, 2015, **45**, 18.
- 24 J. Yu, C. Yang, J. Li, Y. Ding, L. Zhang, M. Z. Yousaf, J. Lin, R.  
 Pang, L. Wei, L. Xu, F. Sheng, C. Li, G. Li, L. Zhao and Y. Hou,  
*Adv. Mater.*, 2016, **26**, 4114.  
 25 S. Shen, S. Wang, R. Zheng, X. Zhu, X. Jiang, D. Fu and W.  
 Yang, *Biomaterials*, 2015, **39**, 67.  
 26 N.-H. Cho, T.-C. Cheong, J. H. Min, J. H. Wu, S. J. Lee, D. Kim,  
 J.-S. Yang, S. Kim, Y. K. Kim and S.-Y. Seong, *Nature*  
*Nanotechnol.*, 2011, **6**, 675  
 27 Y. Kim, Y. S. Choi, H. J. Lee, H. Yoon, Y. K. Kim and M. Oh,  
*Chem. Commun.*, 2014, **50**, 7617  
 28 K.-H. Choi, H.-J. Lee, B. J. Park, K.-K. Wang, E. P. Shin, J.-C.  
 Park, Y. K. Kim, M.-K. Oh and Y.-R. Kim, *Chem Commun.*,  
 2012, **48**, 4591  
 29 C. S. S. R. Kumar and F. Mohammad, *Adv. Drug Deliver. Rev.*,  
 2011, **63**, 789.  
 30 M. C. Urbina, S. Zlnoeva, T. Miller, C. M. Sabllov, W. T.  
 Monroe and C. S. S. R. Kumar, *J. Phys. Chem. C*, 2008, **112**,  
 11102.  
 31 Y. Hou, Z. Xu and S. Sun, *Angew. Chem. Int. Ed.*, 2007, 46,  
 6329  
 32 A. Pineau, N. Kanari, I. Gaballah, *Thermochimica Acta*, 2007,  
**456**, 75  
 33 Y. Sun, B. Zhou, Y. Lin, W. Wang, K. A. S. Fernando, P. Pathak,  
 M. J. Mezziani, B. A. Harruff, X. Wang, H. Wang, P. G. Luo, H.  
 Yang, M. E. Kose, B. Chen, L. M. Veca and S. Xie, *J. Am. Chem.*  
*Soc.*, 2006, **128**, 7756.  
 34 W. Strek, B. Cichy, L. Radosinski, P. Gluchowski, L. Marciniak,  
 M. Lukaszewicz and D. Hreniak, *Light Sci. Appl.*, 2015, **4**,  
 e237.  
 35 J. L. Bredas, R. Silbey, D. S. Boudreaux and R. R. Chance, *J.*  
*Am. Chem. Soc.*, 1983, **105**, 6555.  
 36 A. B. Bourlino, A. Stassinopoulos, D. Anglos, R. Zboril, M.  
 Karakassides and E. P. Giannelis, *Small*, 2008, **4**, 455.  
 37 Q. L. Zhao, Z. L. Zhang, B. H. Huang, J. Peng, M. Zhang and D.  
 W. Pang, *Chem. Commun.*, 2008, **41**, 5116.  
 38 E. Kim, J. Kyhm, J. H. Kim, G. Y. Lee, D. H. Ko, I. K. Han and H.  
 Ko, *Sci. Rep-UK*, 2013, **3**, 3253.  
 39 K. J. Thomas, M. Sheeba, V. P. N. Nampoori, C. P. G.  
 Vallabhan and P. Radhakrishnan, *J. Opt. A: Pure Appl. Opt.*,  
 2008, **10**, 055303.  
 40 P. K. Chu and L. Li, *Mater. Chem. Phys.*, 2006, **96**, 253.

COMMUNICATION

Nanoscale

1  
2  
3  
4

Nanoscale Accepted Manuscript